MAUSAM, **54**, 1 (January 2003), 299-314

551.501.721 : 551.507.362.2

Comparison of radiative fluxes at the top of the atmosphere from INSAT and ERBE

ARINDAM CHAKRABORTY and J. SRINIVASAN

Centre for Atmospheric and Oceanic Sciences,

Indian Institute of Science, Bangalore - 560 012, India

e mail : jayes@caos.iisc.ernet.in

सार – वायुमंडल के ऊपर (टी.ओ.ए.) होने वाले विकिरण अभिवाहों का समुचित ज्ञान होना जलवायु की परिवर्तनशीलता का अध्ययन करने के लिए आवश्यक है। गत 30 वर्षों के दौरान अनेकों भूस्थैतिक उपग्रह अवरक्त और दृश्य क्षेत्रों में संकीर्ण स्पैक्ट्रल बैंड में विकिरण अभिवाहों का मापन कर रहे हैं। ये आँकड़े जलवायु अध्ययनों के लिए उपयोगी सिद्ध होंगे यदि इसे सकल विकिरण अभिवाहों में परिवर्तित किया जा सके। इस शोध पत्र में हमने यह बताया है कि भूविकिरण बजट प्रयोग (ई.आर.बी.ई) से लिए गए आँकड़ों की तुलना भारतीय भूस्थैतिक उपग्रह इनसैट – 1बी से प्राप्त टी.ओ.ए. मासिक माध्य बहिर्गामी दीर्घतरंग विकिरण (ओ.एल.आर.) में त्रुटियाँ अधिकांश क्षेत्रों में 15 Wm^{-2} से कम रही है। इससे पता चलता है कि इनसैट संकीर्ण बैंड अभिवाह से विस्तृत बैंड अभिवाह में परिवर्तन के फलस्वरूप कोई बड़ी त्रुटियाँ नहीं हुई हैं। भारतीय क्षेत्र में जलवाष्प की अधिक मात्रा के कारण ऐसा हो सकता है। यह बताया गया है कि इनसैट ओ.एल.आर. में होने वाली त्रुटि, प्रतिमाह उपलब्ध होने वाले चित्रों की संख्या पर निर्भर करती है। आइसोट्रॉपिक रिफलेक्टेंस अजम्पशन के कारण ई.आर.बी.ई. से तुलना करने पर इनसैट एल्बिडों का महासागर में नकारात्मक बायस रहा है। स्थल में ऐसा कोई बायस नहीं देखा गया। इनसैट में ऐसे निम्न एल्बिडों बायस को महासागर में 2 प्रतिशत के बराबर स्थिर टर्म को जोड़कर समाप्त किया गया। इसमें यह बताया गया है कि यदि एल्बिडों की गणना के लिए प्रतिदिन दो चित्रों का उपयोग किया जाए तो स्वच्छ आकाश एल्बिडों में सूर्य की चमक के प्रभाव को हटाया जा सकता है। इनसैट और ई.आर. बी.ई. के बीच टी. ओ.ए. में कुल विकिरण का अंतर 10 Wm^{-2} तक दिखाया गया है। कुछ क्षेत्रों में, जैसे सउदी अरब (दिसंबर 1988 से मार्च 1989) में दो ई.आर.बी.ई. उपग्रह प्रेक्षेणों (20 Wm^{-2}) के बीच अंतर से ई.आर.बी.ई. और इनसैट से आकलित कुल विकिरण (10 Wm^{-2}) कम पाया गया। इससे यह सपष्ट पता चलता है कि कुल विकिरण का दैनिक परिवर्तन, मासिक कुल विकिरण के औसत आकलन करने में बड़ी त्रुटियाँ उत्पन्न कर सकता है।

ABSTRACT. An accurate knowledge of radiative fluxes at the Top of the Atmosphere (TOA) is necessary to study the variability of climate. Many geostationary satellites have been measuring radiative fluxes in a narrow spectral band in the infrared and visible regions during the past 30 years. This data will be useful for climate studies if it can be converted to total radiative fluxes. In this paper we demonstrate that the errors in monthly mean Outgoing Longwave Radiation (OLR) at the TOA obtained from the Indian geostationary satellite INSAT-1B is less than 15 W m^{-2} in most of the regions when compared to the data from the Earth Radiation Budget Experiment (ERBE). This indicates that the conversion of INSAT narrowband flux to broadband flux does not result in large errors. This could be on account of high water vapour content in the Indian region. The error in INSAT OLR has been shown to be dependent on number of images available per month. INSAT albedo has a negative bias over ocean when compared to ERBE on account of the isotropic reflectance assumption. No such bias was noticed over land. This low albedo bias in INSAT was removed by adding a constant term equal to 2% over ocean. It has been shown that the effect of Sun Glint in clear sky albedo can be removed if two images per day are used for the calculation of albedo. The difference in net radiation at the TOA between INSAT and ERBE has been shown to be within 10 W m^{-2}. In some regions, such as Saudi Arabia (from December 1988 to March 1989) the difference between ERBE and INSAT estimated net radiation (~10 W m^{-2}) was found to be less than the difference between two ERBE satellite observations (~20 W m^{-2}). This indicates clearly that diurnal variation of net radiation can cause large errors in the estimates of monthly mean net radiation.

Key words – INSAT, ERBE, Outgoing longwave radiation, Albedo, Net radiation, Cloud radiative forcing, Remote sensing..

1. Introduction

The variation in the net radiation at the top of the atmosphere (TOA) drives the general circulation of the atmosphere. Estimation of radiation budget from space was initiated nearly 40 years ago. The changes in satellites, sensing instruments and data retrieval algorithms over this period have, however, affected the

accuracy of the data set. Most operational satellites carry a narrow wavelength band pass filter to sense radiation. Some knowledge about the vertical distribution of temperature and humidity is necessary to convert this data to the broadband radiative flux. The measurement of earth radiation budget (ERB) from space using broadband sensors in the Earth Radiation Budget Experiment (ERBE) has revealed many features of interest about the earth's climate, which were found to be quite different from the earlier measurements (Ramanathan *et al*., 1989). In the 1980's, National Aeronautics and Space Administration (NASA), U.S.A., launched the ERBE project (Barkstrom, 1984). The objective of this project was to measure accurately different radiative parameters from space with broad spectral band sensors. Three satellites, *viz*., NOAA9, NOAA10 and ERBS, carried nearly identical sensors to view a region at different times of a day to capture the diurnal variation of radiation. But all the three satellites worked together only for a short span and the consequent temporal sampling deficiency is inherent in ERBE data. Bergman and Salby (1997) have shown that the error in the measurement of monthly mean deep cloud fraction over the tropical continents can be as high as 100% if diurnal variability is not sampled properly. Ramanathan (1987) has illustrated the effect of the equatorial crossing time of polar orbiting satellites on the measurement of zonal mean absorbed solar radiation using a general circulation model. The temporal sampling in ERBE was not adequate but it is still considered as the benchmark for all radiative measurements from space. The archived ERBE data has been used in a variety of climate studies. The Indian Space Research Organisation (ISRO) launched the INSAT series of geostationary satellites beginning in early 1980's. Along with the television broadcasting and telecommunication instruments, sensors were provided on board the INSAT satellites for meteorological purposes. Higher temporal sampling rate is the unique feature of geostationary satellites. INSAT-1B was launched in August 1983 after the first satellite INSAT-1A failed in orbit in September 1982 (Lamm *et al*., 1991). The infrared (IR) and visible detectors of INSAT-1B have provided data with adequately high temporal sampling. However, this data was used mainly for weather prediction and the estimation of large-scale precipitation (Arkin *et al*., 1989). The accuracy of the radiative fluxes at the TOA from INSAT has not been examined so far. The main objective of the present work is to explore the usefulness of INSAT-1B IR and visible data for estimating the radiative fluxes at the TOA.

2. Data

The Very High Resolution Radiometer (VHRR) instrument on board INSAT had two narrowband sensors in the visible and IR regions. The shortwave (SW) half power band pass was at 0.55-0.75 μm. The IR band was at 10.5-12.5 μm (Table 1). The INSAT data used in this study is archived at National Center for Atmospheric Research (NCAR) in Boulder, Colorado (Lamm *et al*., 1991). The data is available with a spatial resolution of 22 km × 22 km near Nadir both for IR and visible images. From April 1988 to March 1989 there were at most 8 IR images per day with nominal acquisition time separated by 3 hours starting at 0000 UTC, and at most 4 visible images per day with nominal acquisition time of 0300, 0600, 0900 and 1200 UTC. Before April 1988 maximum number of images per day were 2 both for IR and visible. In this paper we focus our attention on the period April 1988 to March 1989 since data at a higher temporal resolution is available during this period. The subsatellite point of INSAT-1B was at 74.5° E longitude. When the distance from the subsatellite point becomes large, the satellite zenith angle becomes large and hence accuracy of the radiance data may be affected. Therefore, we have selected the region 40° E-100° E, 30° S - 30° N for this study, which will be termed as Indian region.

TABLE 1

Characteristics of the INSAT and ERBE satellites and their sensors

	ERBE	INSAT-1B
Type	NOAA 09 : polar orbiting	geostationary
	NOAA 10 : polar orbiting	
	ERBS : precessing orbit	
Visible sensor	0.2-5.0 μm	0.55-0.75 μm
IR sensor	5.0-50.0 μm	10.5-12.5 μm
Total range sensor	0.2-50.0 μm	–
Sampling	NOAA 09 : 0230,1430 local time NOAA 10 : 0730,1930 local time ERBS : variable	0000, 0300, 0600, 0900, 1200, 1500, 1800, 2100 GMT

Radiative fluxes obtained from INSAT have been compared with that of the ERBE satellites. The scanning radiometer (SR) of the ERBE satellites had broadband channels at visible (0.2-5.0 μm) and IR (5.0-50.0 μm) regions, as well as a total spectrum channel at 0.2-50.0 μm (Barkstrom *et al*., 1989). Existence of broadband channel provided more accurate estimates of radiative quantities at the TOA. We used ERBE S-4 data product (Barkstrom *et al*., 1989) which comprises monthly 2.5° × 2.5° longitude-latitude box average scanner measurements. Fig 1 shows the time series of outgoing longwave radiation (OLR) and albedo from the ERBE satellites averaged over the Indian

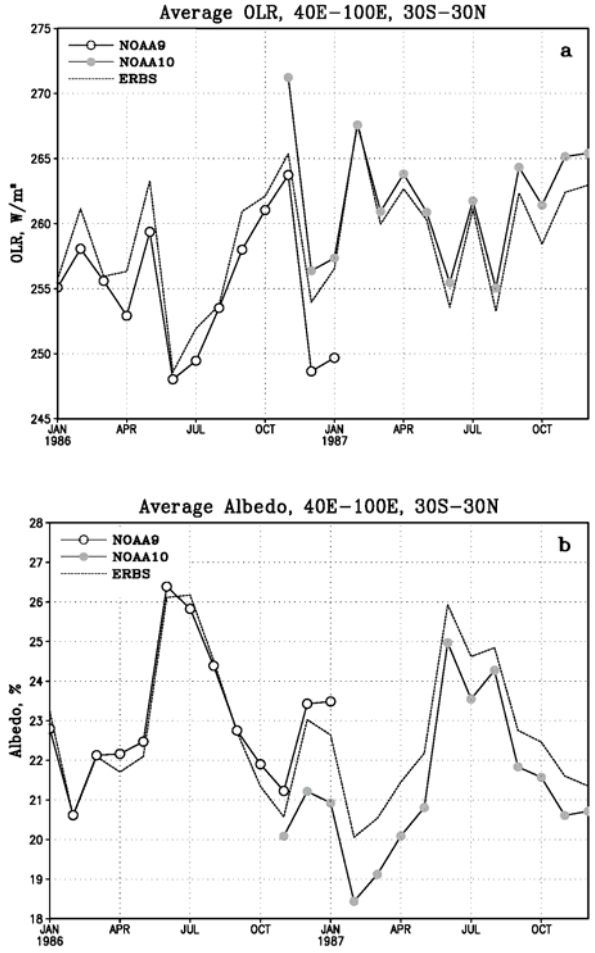

Figs. 1 (a&b). Time series of monthly mean (a) OLR and (b) albedo obtained from NOAA9, NOAA10 and ERBS averaged over the Indian region

region. There is a negative bias in NOAA9 and positive bias in NOAA10 when compared to ERBS estimates of OLR. Biases are of the opposite sign for albedo. Kyle *et al*. (1993) argued that diurnal sampling simplifications should be the largest source of error between the ERBE satellites. NOAA9 and NOAA10 were in sun-synchronous orbit with fixed equatorial crossing time. Therefore, data collected by these two satellites is biased according to their time of transit over any place. The third ERBE satellite, ERBS was in a non-synchronous orbit with a drift in equator crossing time during different passes. Taking into account both ascending and descending nodes, ERBS precessed through all local hours at a place in 36 days (Harrison *et al*., 1988). Therefore, on a monthly mean scale ERBS data should not suffer from diurnal sampling bias. Therefore, we consider ERBS estimated radiative fluxes to be the benchmark in this paper.

TABLE 2

RMS error (Wm^{-2}) in ERBS-INSAT OLR and clear sky OLR for July 1988 and January 1989 averaged over the Indian region for the two sets of narrowband to broad band conversion

	New constants		Old constants	
	Jul 1988	Jan 1989	Jul 1988	Jan 1989
OLR	10.7	8.2	19.1	18.2
Clear sky OLR	11.8	7.2	25.7	25.2

3. Outgoing longwave radiation

INSAT IR data was in the form of brightness temperature (T_b) which is defined as the equivalent blackbody temperature emitting the same radiance as that sensed by the satellite. We converted this IR radiance to wavelength integrated OLR using the relations from Abel and Gruber (1979):

$$T_f = (a + bT_b)T_b \quad (1a)$$

$$OLR = \sigma T_f^4 \quad (1b)$$

where $\sigma = 5.67 \times 10^{-8}$ Wm^{-2} K^{-4}, is the Stefan-Boltzmann constant; T_f is called the flux equivalent temperature; a and b are constants of the equation, which depend on factors like the response function of the sensor used and vertical water vapour distribution. Arkin *et al*. (1989) have suggested the following numerical values of a and b at zero satellite zenith angle

$$a = 1.1889 \quad (2a)$$

$$b = -0.000989 \quad (2b)$$

Magnitude of both the constants decrease as satellite zenith angle increases. Arkin *et al*. (1989) at first averaged the pixel brightness temperature to a 2.5°×2.5° longitude-latitude grid box and then used the Eqn. (1) to calculate the OLR. As the equations for the conversion of narrowband to broadband fluxes are highly nonlinear, this may cause substantial underestimate of OLR if the variability of the scene type is high (Gruber *et al*., 1983) within a 2.5°×2.5° box. Therefore, we have calculated the OLR of the individual pixels at first and then averaged over a 2.5°×2.5° longitude-latitude box to get the OLR of that box. We found that the variation of a and b with satellite zenith angle did not cause large errors since the satellite zenith angle was below 50° in the Indian region. Therefore we have used the nadir values cited above for the conversion of brightness temperature to flux

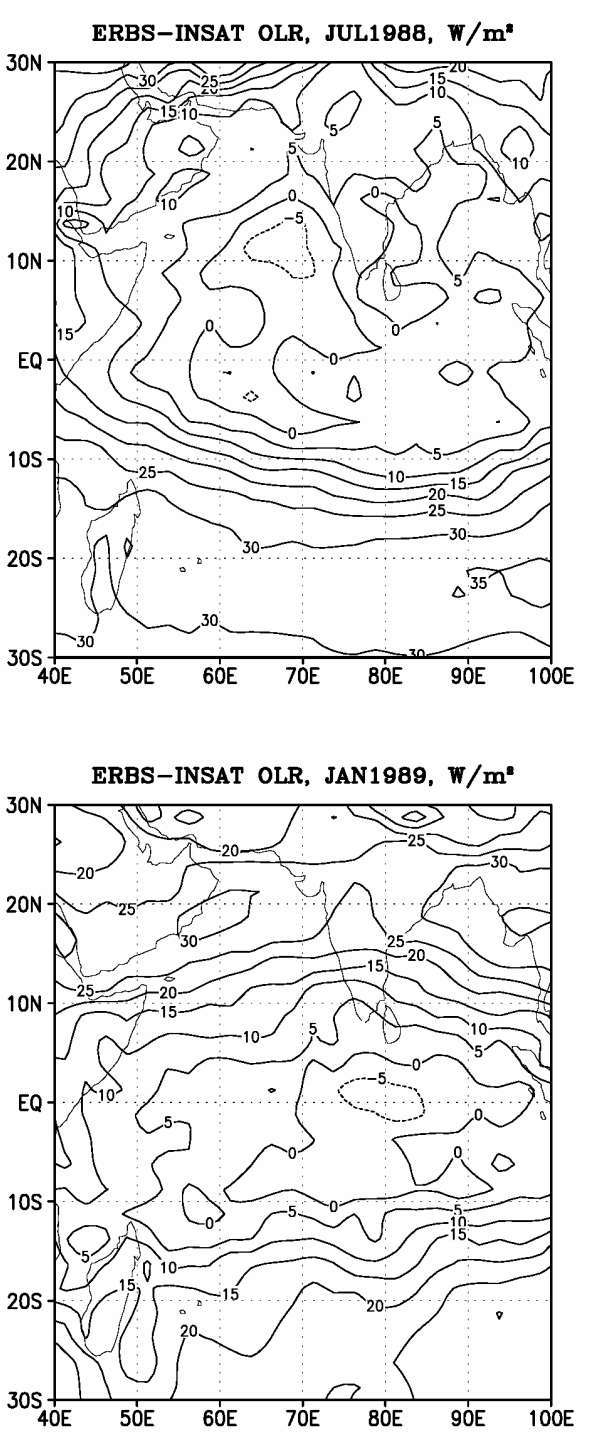

Fig. 2. Difference between ERBS and INSAT OLR for July 1988 and January 1989. INSAT OLR was calculated using the regression constants after Arkin *et al*. (1989)

temperature. Fig 2 shows the difference between ERBS and INSAT OLR for July 1988 and January 1989. INSAT OLR was calculated using the constants given in Eqn. (2). Large differences are found between ERBE and INSAT

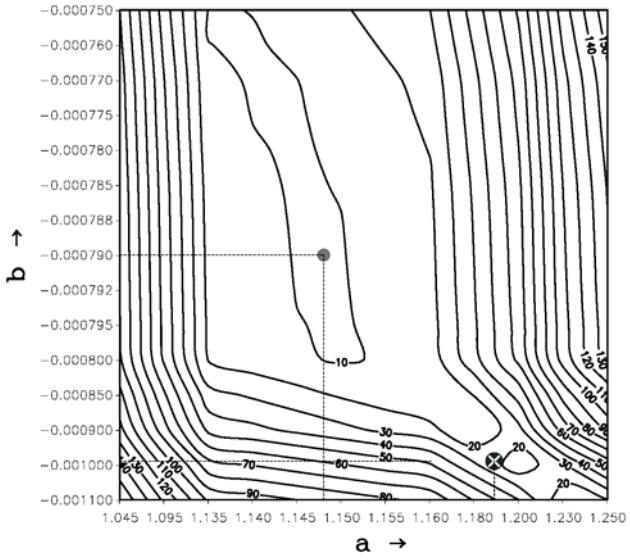

Fig. 3. RMS error of ERBS-INSAT OLR for the month of May 1988 in the (a,b) plane. The filled circle shows the position of (a,b) selected for our study and the crossed circle shows the position of the old set. a and b axes are zoomed in at the middle

OLR in most of the regions. Errors are relatively less in the cloudy regions. The root mean square (RMS) error averaged over the Indian region for these two months was 19.1 and 18.2 Wm^{-2} respectively (Table 2). The RMS errors are larger than the errors inherent in the ERBE data. We have used an empirical technique to reduce this error. We have achieved this goal by adjusting the values of a and b in Eqn. (2). OLR was calculated using the Eqn.(1) for every pixel and averaged over a 2.5° box for every images. Average over all the images of a month gave the monthly mean OLR for that grid box for that month. We selected May 1988 for our empirical method for finding a and b. RMS error for every grid box was calculated with respect to ERBS data for that month and area mean RMS error was calculated for one set of regression constants. We repeated the whole procedure for a possible range of values of a and b. Examination of the variation of RMS error with a and b indicated a region where the RMS error was a minimum. The result is shown in Fig. 3. Note that the axes are zoomed in at the middle region. A valley of minimum RMS error (< 10 Wm^{-2}) is clearly indicated. Selection of values of a and b from this region should give the lowest error. We have chosen the values given below.

$$a = 1.1480 \quad (3a)$$

$$b = -0.000790 \quad (3b)$$

These values ensure that the RMS error is almost same when we consider the difference between ERBS and INSAT OLR in both low and high OLR regions. The

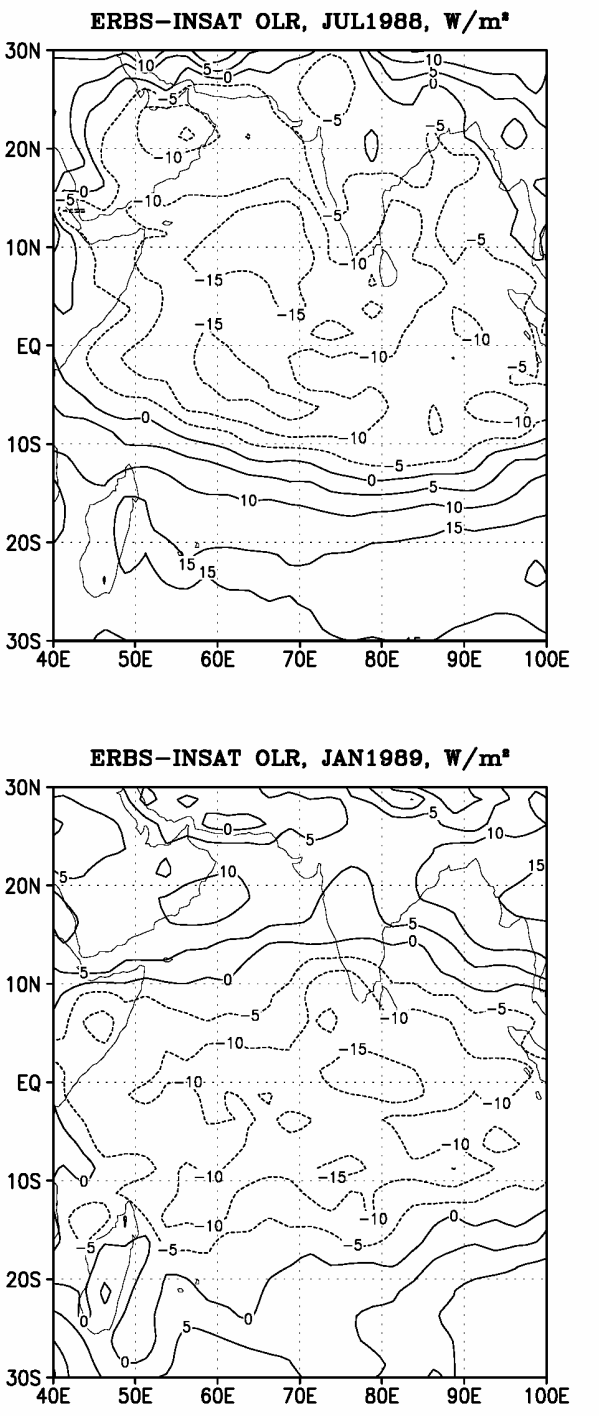

Fig. 4. Difference between ERBS and INSAT OLR for July 1988 and January 1989. INSAT OLR was calculated using the regression constants obtained from the present empirical method

values of a and b chosen by this method is shown as a filled circle in Fig 3. The values of a and b used by Arkin *et al*. (1989) is shown as a crossed circle. Henceforth we

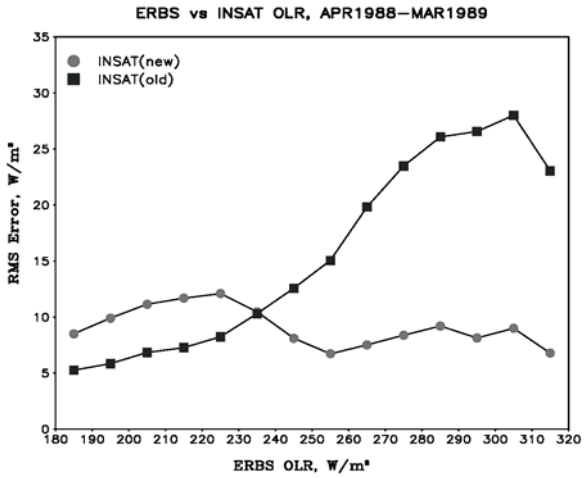

Fig. 5. RMS error of the INSAT OLR as a function of ERBS OLR

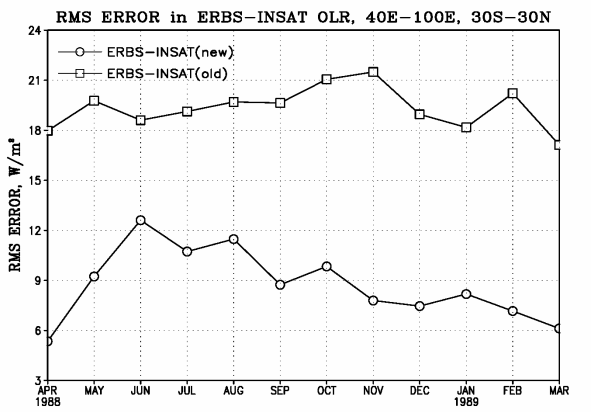

Fig. 6. Time series of RMS error between ERBS and INSAT OLR

will call the present empirically derived constants as new set and those used by Arkin *et al*. (1989) as old set. Fig. 4 shows the difference between the ERBS and INSAT OLR for July 1988 and January 1989, where INSAT OLR was calculated using the new set of regression constants. Comparing with Fig. 2 one can notice the substantial improvement in OLR estimation from INSAT using the new constants. Area average RMS error has been reduced by about 10 Wm^{-2} in these two months when compared with the INSAT(old) (Table 2). Errors in different OLR ranges was calculated as follows: INSAT OLR from April 1988 to March 1989 were grouped into different bins of size 10 Wm^{-2} based on the corresponding ERBS OLR value. RMS of ERBS-INSAT OLR was calculated and bin average was obtained. The result is shown in Fig. 5. Note that the RMS error is high for the old set when OLR is above 240 Wm^{-2}. On the other hand, RMS error obtained by using the new constants is around 7 Wm^{-2} except in the range 195-235 Wm^{-2} where it is around 12 Wm^{-2}. Since the accuracy of ERBS is around 5 to 10 Wm^{-2}, we can conclude that the INSAT OLR obtained by the new method is as good as ERBS data set. Fig. 6 shows that

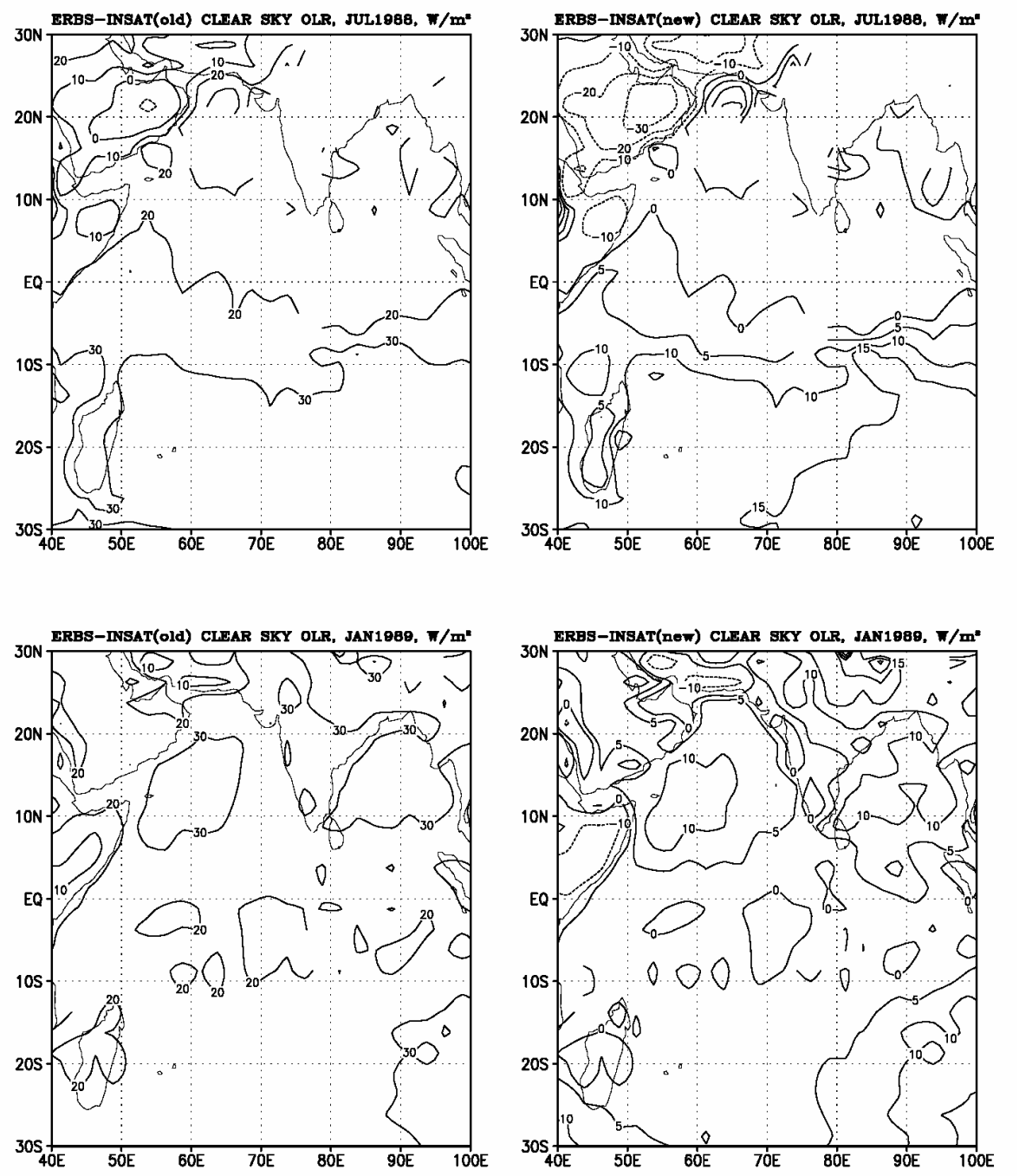

Fig. 7. ERBS-INSAT clear sky OLR for the two sets of regression constants in July 1988 and January 1989

RMS error in INSAT(new) is in the range 6 to 13 Wm^{-2} while for INSAT(old) is around 18 to 21 Wm^{-2}. RMS error for INSAT(new) is as low as 6 Wm^{-2} for March 1989 when we have highest number of images (243 in total) and as high as 13 Wm^{-2} for June 1988 when we have lowest number of images (154 in total). The need of large temporal sampling is quite evident from this result.

4. Clear sky OLR

Another important radiative parameter is the spectrally integrated longwave (LW) flux at the TOA under clear sky conditions, termed as clear sky OLR. Accurate knowledge of clear sky OLR is needed to study cloud radiative forcing (CRF). We calculated monthly

mean clear sky OLR from INSAT IR data using the following algorithm,

(*i*) Consider 10 pixels of every image with highest brightness temperature from a 2.5°×2.5° longitude-latitude box.

(*ii*) Calculate the standard deviation (SD) of these pixels with reference to the surrounding 8 pixels.

(*iii*) If SD is less than 1.0 K, the pixel is declared as clear.

(*iv*) Use Eqn. (1) and (3) to calculate spectrally integrated LW flux from every clear pixel and average over all the clear pixel from that grid box for that image.

(*v*) Average over all the images of a month to get the representative clear sky OLR of that month.

The first condition was needed to exclude the pixels with deep clouds because brightness temperature of deep clouds is less. But the pixels with low altitude clouds still remain under consideration since the temperature of low altitude clouds is not very different from the surface temperature. We eliminate these pixels with the 2nd and 3rd conditions. If a scene is uniformly clear, all the pixels in that scene will have nearly equal brightness temperature, unless the underlying surface type changes vary rapidly. A rather difficult situation arises in the overcast condition when there is no clear pixel in a 2.5° box. But as the clear sky fluxes are significantly more homogeneous than overcast fluxes (Ramanathan *et al*., 1989), the SD of these pixels will be higher than pixels from uniformly clear scene. Therefore, the third condition will eliminate most cloudy pixels.

Fig 7 shows the difference between ERBS and INSAT estimated clear sky OLR for the two sets of constants of narrowband to broadband conversion for July 1988 and January 1989. Improvement of about 15-20 Wm^{-2} in the estimates can be noticed in most of the places using the new constants. Higher error of INSAT(new) in Saudi Arabian desert and south Indian Ocean in July 1988 may be attributed to the limitations in the single-channel narrowband to broadband conversion, as pointed out by Gruber *et al*. (1994) who compared estimated OLR from NOAA AVHRR narrowband data with that of the ERBE estimations. We found particularly low error at regions where water vapour content of an atmospheric column is high. Saudi Arabia and South Indian Ocean is characterized by low water vapour in July and hence errors are high at these two regions. Area average RMS error for July 1988 is 11.8 and 25.7 Wm^{-2} respectively for the new and old constants (Table 2). Similar improvements are seen in the other months as well.

5. Longwave cloud radiative forcing

The effect of cloud on radiation budget can conveniently be described by cloud radiative forcing. Clouds absorb the LW radiation emitted by the warmer earth and emit LW radiation at a colder temperature of the cloud top. Hence, presence of cloud reduces the amount of emission of LW radiation to the space, which causes LW warming. This is termed as longwave cloud radiative forcing (LWCRF) which can be written as

$$LWCRF = F_{clr} - F \quad (4)$$

where F_{clr} and F are OLR in clear sky and all-sky conditions respectively. As $F_{clr} > F$, LWCRF is positive in general.

Fig. 8 shows the spatial distribution of LWCRF from ERBS, NOAA10, INSAT(old) and INSAT(new) for July 1988. The pattern is same for all the four data sets. INSAT(new) is closer to ERBS in the tropical convergence zone (TCZ) than INSAT(old) value. Error in INSAT(old) LWCRF is not as much as the individual error in F and F_{clr} because of the cancellation of bias of the same sign. Same feature is noticed in January 1989 as well. Note that INSAT is able to provide CRF data in the regions where ERBS has no data. This is because the method used to identify clear skies from ERBE data was very stringent and hence did not find many clear pixels in the Indian monsoon region with samples twice per day.

6. Albedo

The narrow band albedo of INSAT in the visible region (0.55-0.75 μm) was converted to broadband albedo by Lamm *et al.* (1991) based on June 1988 INSAT measurements and calibrated measurements from a prior U.S. geosynchronous satellite GOES-1 which was used over the Indian Ocean to support the 1979 Monsoon Experiment (MONEX). For the conversion, diffuse-isotropic reflectance was assumed and the relationship between the narrowband and broadband albedo was considered to be a linear transform. Two 5°×5° regions were taken as the representative of the total region. One was over the central Arabian Sea, centered at 65.0° E and 15.0° N, representing a region free of clouds. The second one was the empty quarter of Arabian Peninsula, centered at 47.5° E and 20.0° N, representing high albedo region. In these regions Smith (1984) provided diurnally varying broadband albedo estimates for GOES-1 data averaged for 10 day periods during1979 monsoon. INSAT visible data set during 1-10 June 1988 was used to get the regression constants of the linear fit between narrowband and broadband albedo. INSAT albedo data that was available for this study was converted to broadband using the above

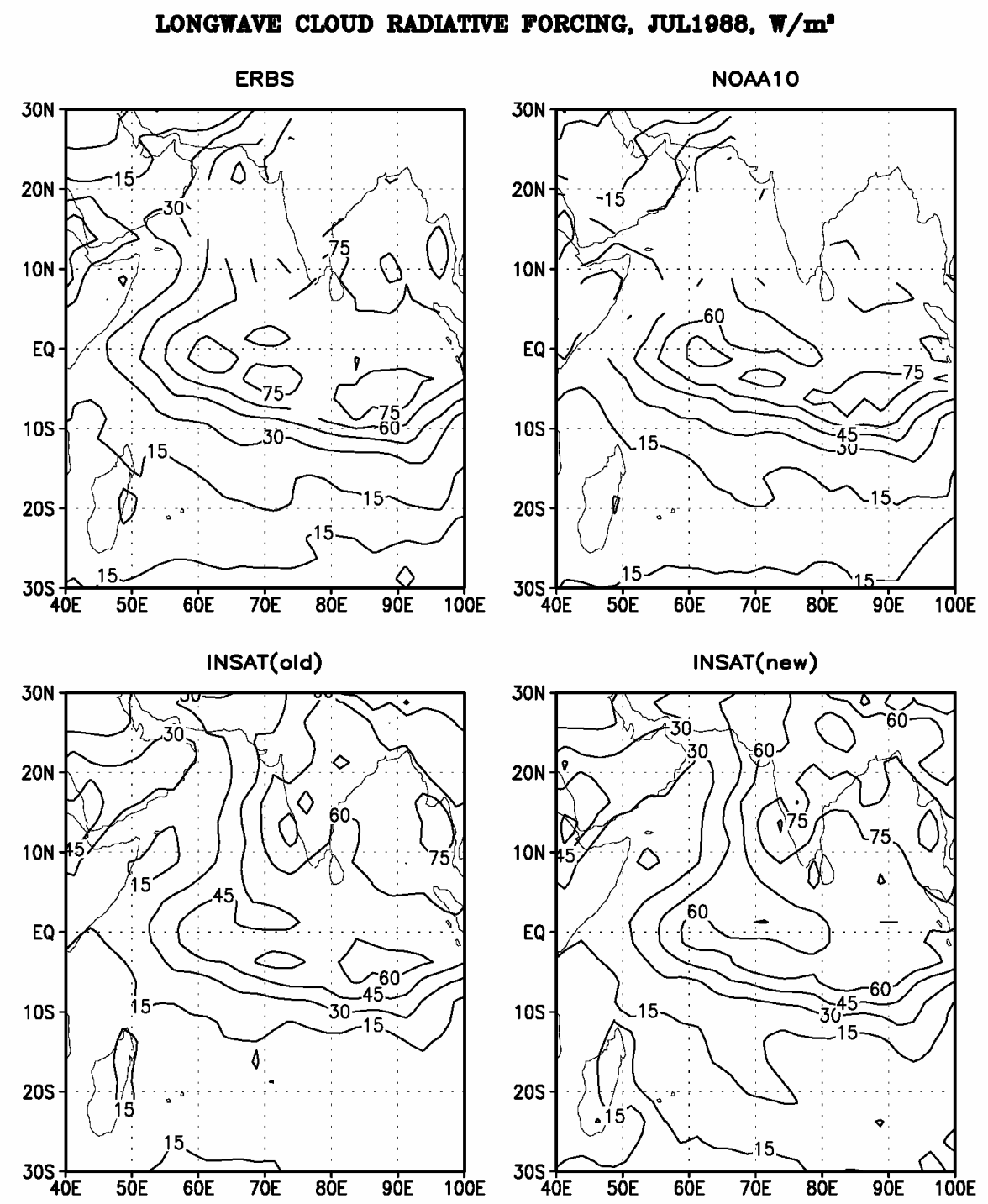

Fig. 8. Longwave cloud radiative forcing from ERBE and INSAT for July 1988

mentioned procedure. There were at most 4 visible images per day April 1988 onwards. The Indian region was partially covered by sunlight in the 0300 and 1200 GMT images. Hence, we used 0600 and 0900 GMT images for our study.

Fig. 9 shows the difference between ERBS and INSAT albedo for July 1988 and January 1989. It is clear from the figure that INSAT albedo is lower than ERBS albedo particularly over ocean. This low albedo bias of INSAT is present in the other months as well. Overall bias

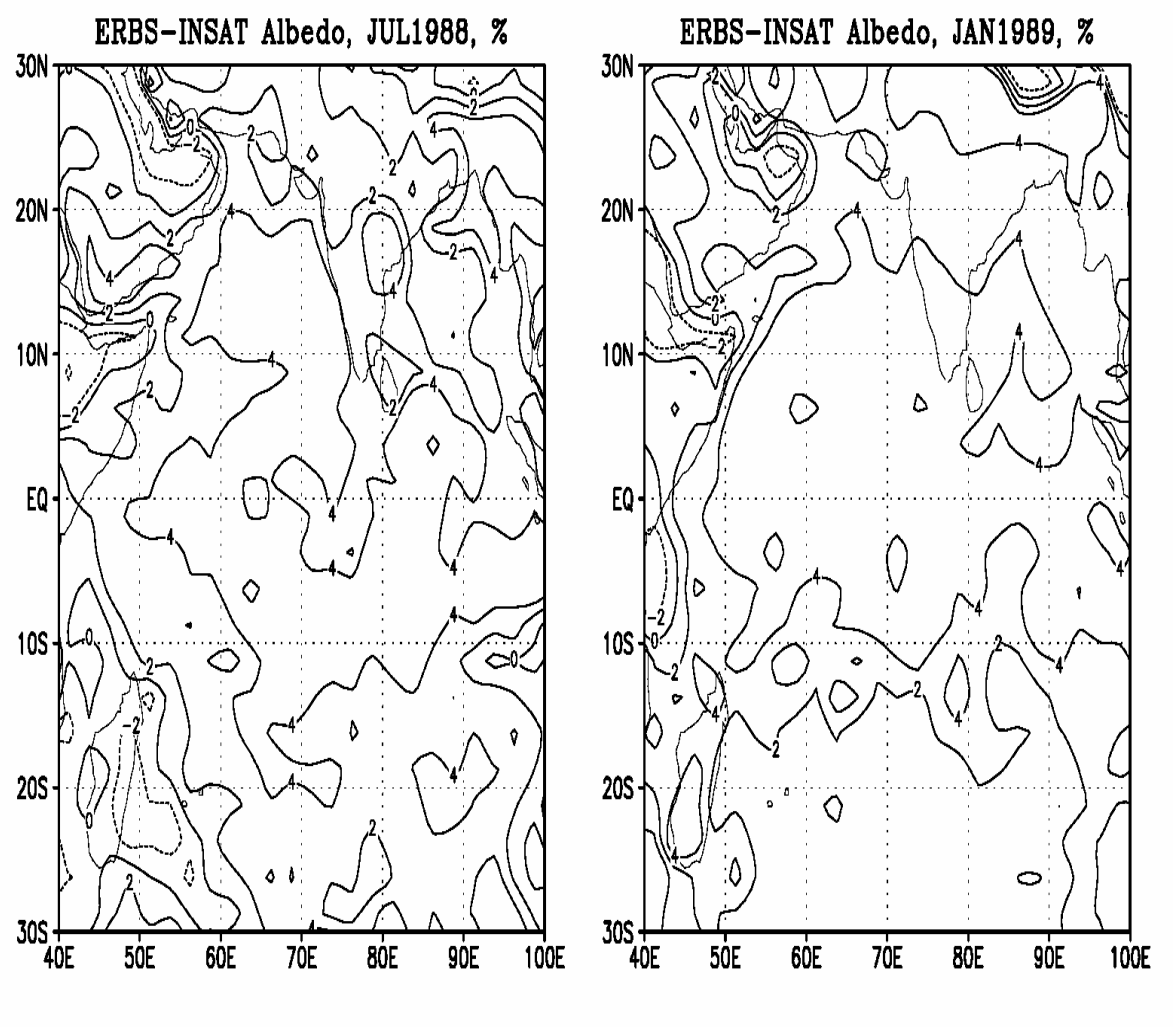

Fig. 9. ERBS-INSAT albedo for July 1988 and January 1989

is about 2% over ocean. Moreover, this bias is not a function of either ERBS or INSAT albedo. Therefore, we have removed this low albedo bias of INSAT by adding a constant term equal to 2% over ocean. We did not correct the albedo over land because the errors in albedo were both positive and negative and a complex function of the different surface types. In Fig. 10 we have plotted the RMS error of INSAT albedo at different bins of ERBS albedo over ocean. INSAT(new) indicates the bias corrected data. It can be noticed that bias correction has decreased the RMS error between ERBS and INSAT albedo in almost all ranges. RMS error has increased slightly at very low albedo. It was found that error in albedo can be reduced substantially if two images per day (0600 and 0900 GMT) are used for the calculation instead of any single image. For example, RMS error in bias corrected INSAT albedo (with respect to ERBS) for April 1988 in the region 55° E - 65° E, 0°-10° N was reduced by

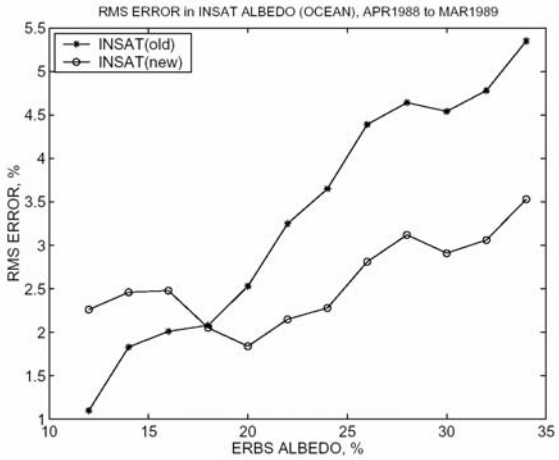

Fig. 10. RMS error between ERBS and INSAT albedo over ocean at different bins of ERBS albedo with and without adding 2%

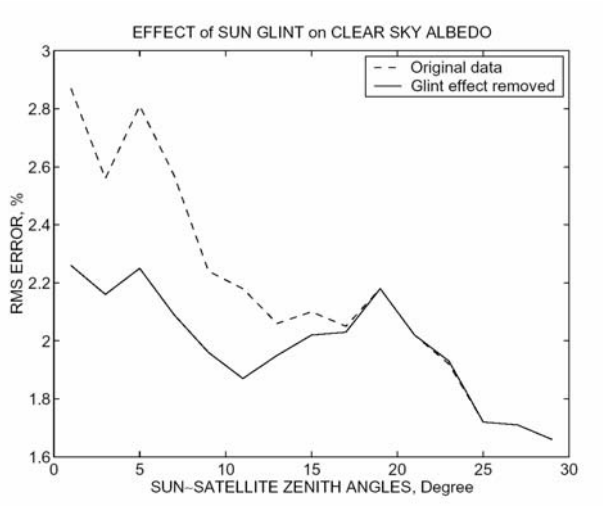

Fig. 11. RMS error in clear sky albedo as a function of the difference between solar and satellite zenith angles over ocean for the period April 1988 to March 1989 in the Indian region

3.5% when we used both the images instead of only 0900 GMT image. The reduction in error on account of the use of two images is due to the automatic elimination of sun glint effect. This is discussed in the next section.

7. Clear sky albedo

Albedo under the clear sky condition is a direct representative of the surface type-atmospheric effect is small for SW radiation and should show a clear dependence on the surface property and the angles of measurements. Moreover, clear sky albedo helps us to understand the effect of albedo on CRF. Reflectivity of cloud is more than the reflectivity of land or ocean surfaces and temperature of cloud top is generally less than that of the surface. Therefore clear sky albedo should be less than all-sky albedo and clear sky brightness temperature should be more than all-sky brightness temperature. We focus mainly on these features to develop two algorithms to find monthly mean clear sky albedo from INSAT pixel data. We call these algorithms as 'Standard Deviation (SD) method' and 'Rank method'. The SD method is a uni-spectral technique where we take the lowest 5 albedo of a pixel from all available images of the month, calculate the SD of those pixels with the surrounding pixels which are in the same scene type (land or ocean; we distinguish between scene types due to the sharp variation of albedo over land and ocean). If the SD is less than 1.0%, we considered the pixel as clear. Average over all the clear pixels from a month within a 2.5° box gives the clear sky albedo of that box for that month.

In the Rank method, both the IR and visible images were used to identify clear sky. As the units of IR brightness temperature and albedo are different, we introduced a procedure to allocate rank. At first we ranked all 0600 and 0900 GMT pixel images from lowest to highest albedo value. We rank the corresponding IR images from the highest temperature to the lowest. Now these two ranks were added to get a single cumulative rank. The lower the cumulative rank the more probable that the pixel was clear. We considered five pixels ranked lowest to calculate average monthly mean clear sky albedo. We did not add any bias term to INSAT clear sky albedo data.

The effect of Sun Glint was noticed in clear sky albedo as shown in Fig. 11. Here we have plotted the RMS error between INSAT and ERBS clear sky albedo as a function of the absolute difference between the solar and satellite zenith angles of a grid box. 0600 and 0900 GMT images were taken separately to calculate INSAT clear sky albedo using SD method. The dashed curve indicates the original data where all points over ocean were considered. This shows a high RMS error in INSAT clear sky albedo when the difference between the solar and satellite zenith angles is low. This is because of the unusual high INSAT clear sky albedo caused by the near-specular reflection of ocean surfaces when solar and satellite zenith angles are nearly same. We can remove the glint effect by excluding the points from our calculation for which relative azimuth angle is more than 120°, absolute difference between solar and satellite zenith angles is less than 20° and the clear sky albedo value is greater than the mean of albedo over ocean for that month. By definition, with the first two conditions we have selected the sun glint region approximately. But all the pixels falling in that region may not suffer these specular reflection phenomena because the shape and size of the glint area itself will change with the relative position of the sun and the satellite and also with the degree of roughness of ocean surface. Therefore, we have employed the third criteria to remove only glint-affected pixels from that region. The solid curve of Fig. 11 shows the results after employing the above mentioned criteria to remove glint-affected pixels. Note that the RMS error in clear sky albedo decreases substantially when the difference between solar and satellite zenith angle is low.

The effect of sun glint also can be eliminated using more than one image for calculation. In Fig. 12 we have shown the difference between ERBS and INSAT estimated clear sky albedo over ocean for December 1988. INSAT clear sky albedo was calculated using SD method. At first 0600 and 0900 GMT images were taken separately for the calculation [Figs.12(a&b)],which show a high error of about -6% in the glint affected area when compared to

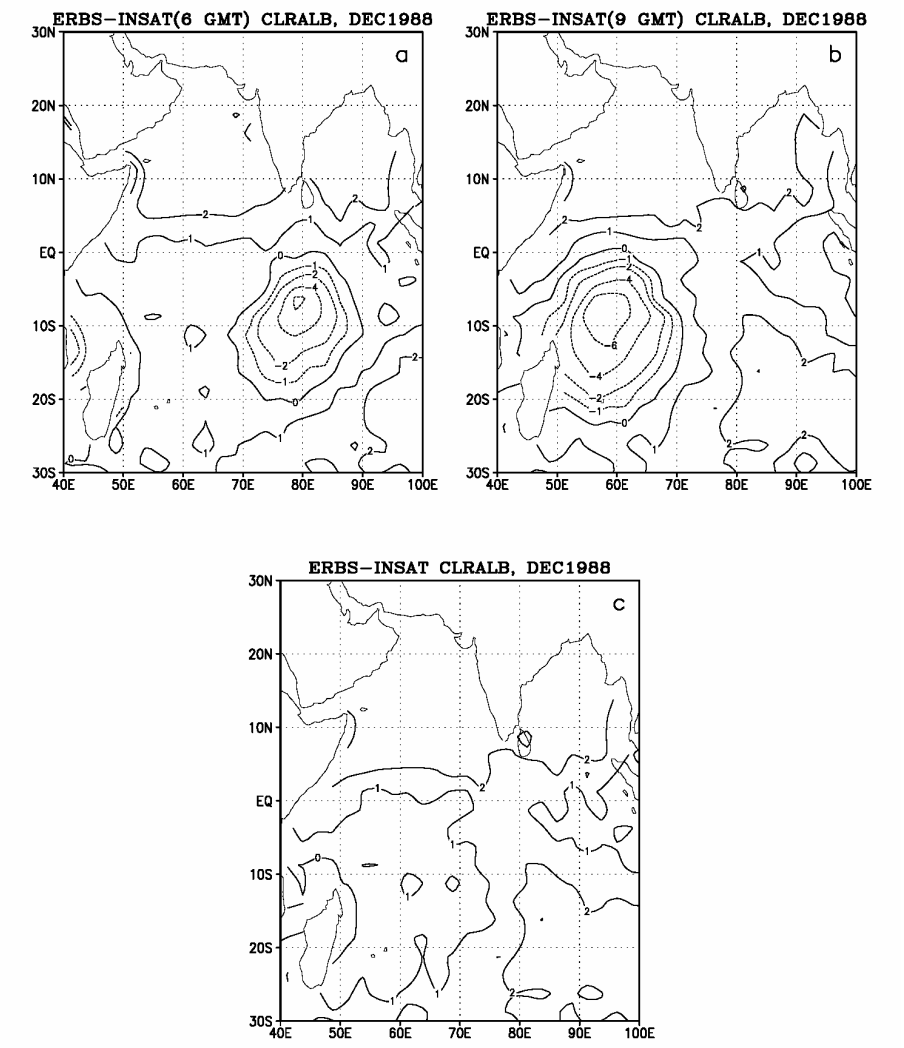

Figs. 12(a-c). Difference in clear sky albedo between ERBS and INSAT in December 1988 for different combinations of INSAT visible images: (a) 0600 GMT, (b) 0900 GMT and (c) 0600 & 0900 GMT combined

ERBS data. When both 0600 and 0900 GMT images were considered, the error has reduced substantially Fig. 12(c). This is due to the fact that our clear sky identification algorithm automatically eliminates glint affected high albedo valued INSAT pixels when data of two different images are available. Therefore, henceforth, we use combined 0600 and 0900 GMT images for INSAT clear sky albedo calculation. In Table 3 we have listed mean clear sky albedo from ERBS and INSAT separately over land and ocean for 4 months. The Table shows that both over land and ocean INSAT clear sky albedo estimated using the Rank method is closer to ERBS data than the SD method. This shows the usefulness of multichannel measurements to identify clear sky. Comparison of Fig. 12(c) with Fig. 9 points out the demerits of isotropic reflectance assumption in all sky conditions. In both the figures INSAT data without bias correction was used. It

TABLE 3

Clear sky albedo over land and ocean from ERBS and INSAT. INSAT clear sky albedo was derived using two separate algorithms (SD method and RANK method)

	Jul 1988	Sep 1988	Dec 1988	Mar 1989
	40° E-100° E, 30° S-30° N : Land			
ERBS	20.2	20.4	21.5	20.2
INSAT (SD)	19.0	17.6	18.0	18.0
INSAT (RANK)	21.0	18.9	19.1	19.0
	40° E-100° E, 30° S-30° N : Ocean			
ERBS	11.6	10.7	10.8	10.2
INSAT (SD)	10.3	9.7	9.1	9.1
INSAT (RANK)	10.9	10.1	9.5	9.4

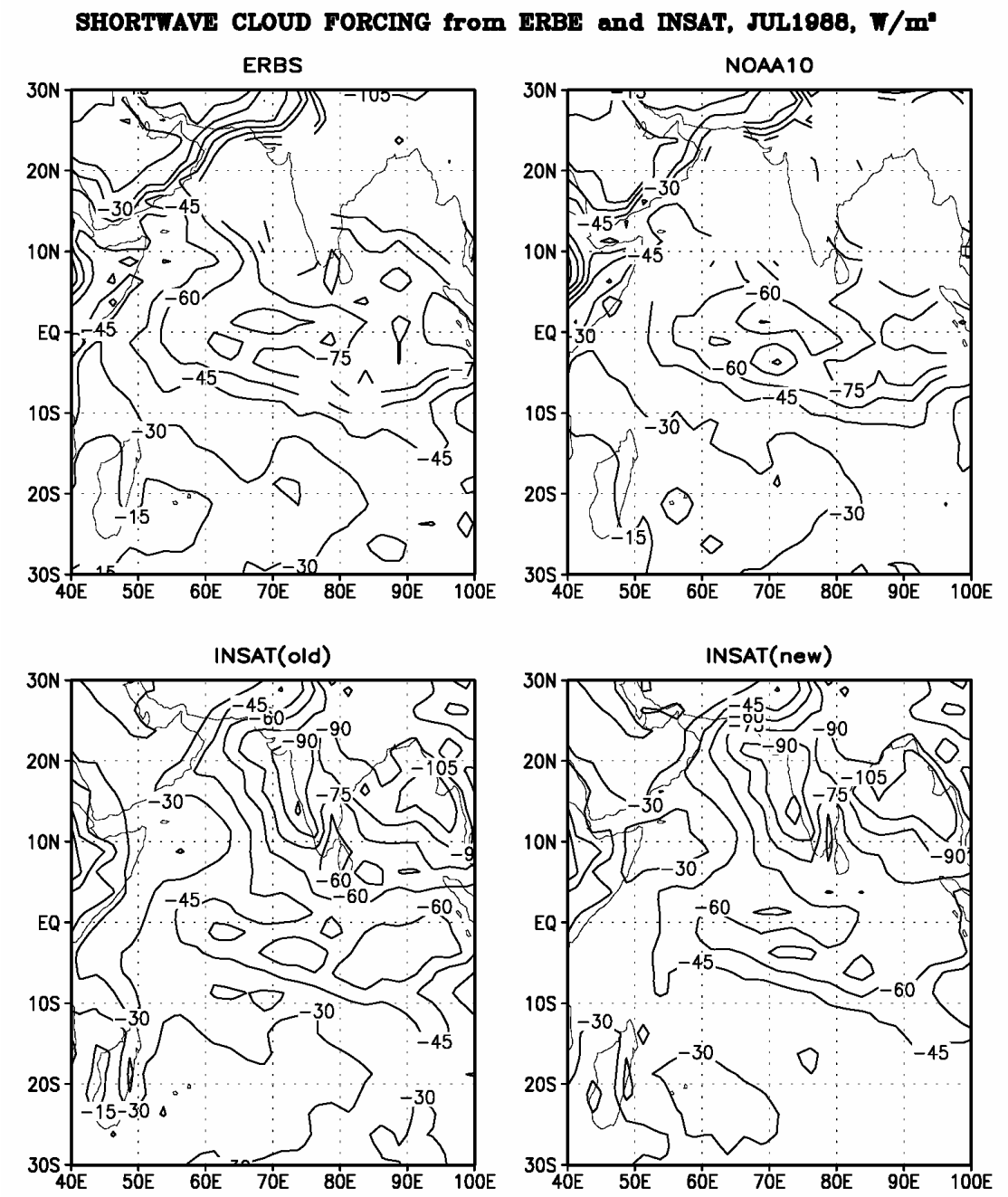

Fig. 13. Shortwave cloud radiative forcing from ERBE and INSAT for July 1988

can be noticed that for clear sky albedo Fig. 12(c) there is less bias in INSAT when compared to ERBS as opposed to the all sky case (Fig. 9). This can be attributed to the highly non-isotropic reflection from cloud surfaces for which isotropic reflection is a very crude assumption. On the other hand, over clear ocean surface the same assumption seems reasonable. Therefore, a large part of the errors in INSAT all sky albedo should be on account of the isotropic reflection assumption for solar radiation.

8. Shortwave cloud radiative forcing

Cloud reflects a large amount of SW radiation coming from the sun. Due to the presence of clouds,

TABLE 4

RMS error in (a) net radiation, (b) absorbed solar radiation and (c) OLR, all in W m^{-2}, for three selected sub-regions. INSAT(new) is not tabulated in (b) over the Saudi Arabian region because INSAT albedo bias was not corrected over land

(a) Net radiation, Wm^{-2}

	Jul 1988	Sep 1988	Dec 1988	Mar 1989
	45° E-55° E, 15° N-25° N : Saudi Arabia			
NOAA10	5.8	3.6	13.3	9.8
INSAT(old)	20.0	17.9	22.0	19.1
INSAT(new)	14.6	10.9	7.8	7.9
	85° E-95° E, 5° N-15° N : Bay of Bengal			
NOAA10	6.6	4.1	4.0	3.8
INSAT(old)	14.3	18.6	23.1	22.3
INSAT(new)	6.4	4.8	3.0	5.7
	75° E-85° E, 25° S-15° S : South Indian Ocean			
NOAA10	3.0	3.4	12.4	9.4
INSAT(old)	40.8	45.6	31.5	30.8
INSAT(new)	17.8	20.9	5.0	6.4

(b) Absorbed Solar Radiation, Wm^{-2}

	Jul 1988	Sep 1988	Dec 1988	Mar 1989
	45° E-55° E, 15° N-25° N : Saudi Arabia			
NOAA10	4.8	4.4	10.6	12.3
INSAT(old)	12.2	9.4	5.8	9.9
	85° E-95° E, 5° N-15° N : Bay of Bengal			
NOAA10	6.8	7.5	4.4	4.1
INSAT(old)	10.8	15.5	6.0	4.4
INSAT(new)	6.2	7.4	4.1	5.1
	75° E-85° E, 25° S-15° S : South Indian Ocean			
NOAA10	2.9	4.1	10.9	9.1
INSAT(old)	9.6	18.2	6.0	11.1
INSAT(new)	4.1	10.9	7.2	5.1

(c) OLR, Wm^{-2}

	Jul 1988	Sep 1988	Dec 1988	Mar 1989
	45° E-55° E, 15° N-25° N : Saudi Arabia			
NOAA10	2.3	2.3	2.9	3.1
INSAT(old)	12.8	20.4	18.5	11.3
INSAT(new)	8.5	4.3	3.8	6.6
	85° E-95° E, 5° N-15° N : Bay of Bengal			
NOAA10	2.9	4.9	2.4	1.2
INSAT(old)	5.6	4.1	18.3	18.7
INSAT(new)	6.2	7.8	2.1	2.7
	75° E-85° E, 25° S-15° S : South Indian Ocean			
NOAA10	0.4	2.2	2.3	1.7
INSAT(old)	31.4	27.7	27.7	21.0
INSAT(new)	14.4	10.4	8.9	5.0

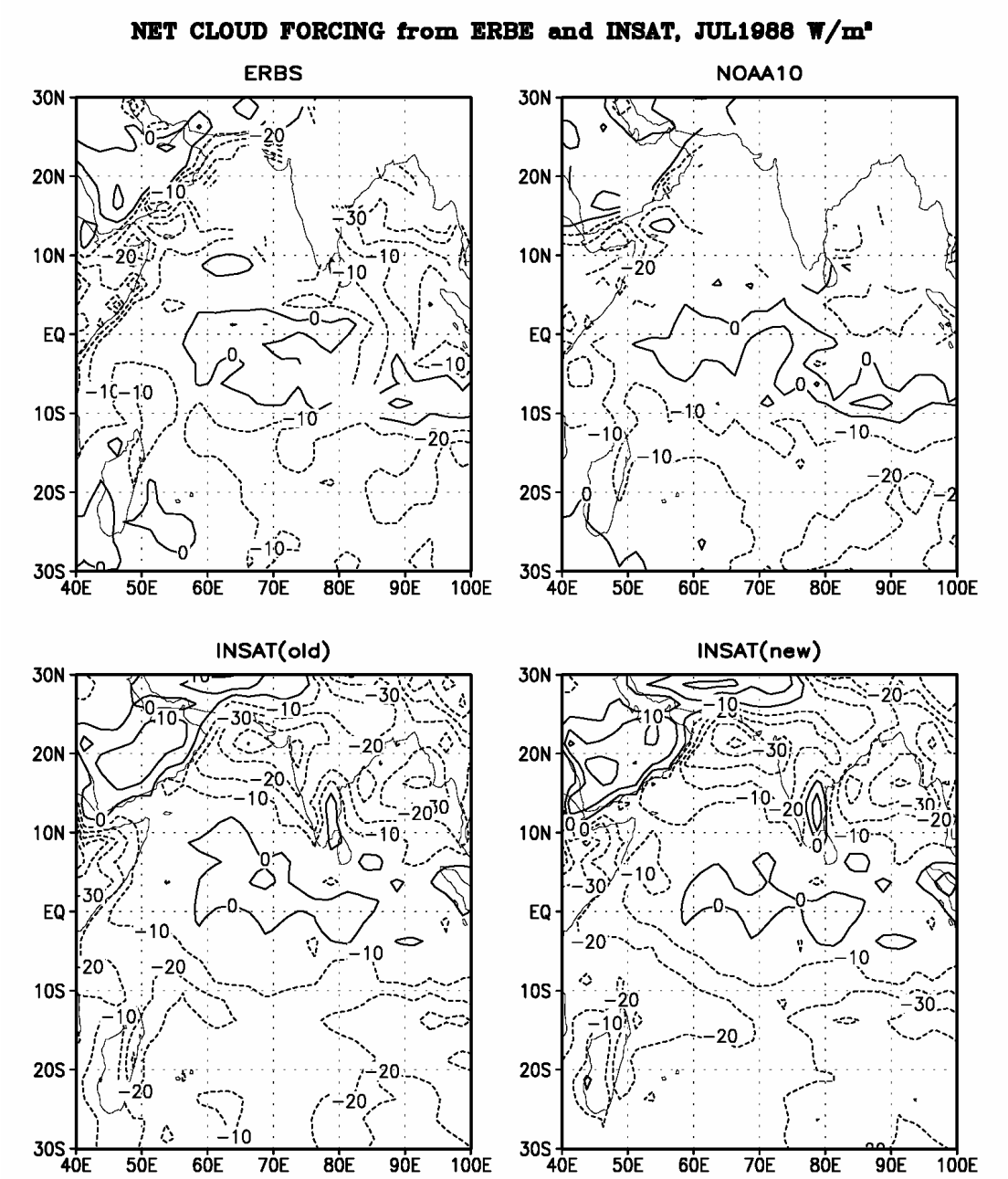

Fig. 14. Net cloud radiative forcing from ERBE and INSAT for July 1988

albedo of the earth is twice of that it would have been in the absence of clouds. Therefore, effect of cloud on the SW radiation is cooling the earth-atmosphere system. Quantitative measurement of this effect is described by shortwave cloud radiative forcing (SWCRF) which is the difference between the clear sky and cloudy sky reflected SW fluxes:

$$SWCRF = S(\alpha_{clr} - \alpha) \quad (5)$$

where α_{clr} and α are albedo at clear sky and all-sky conditions respectively and S is the incoming solar radiation. As $\alpha_{clr} < \alpha$ in general (one exception is fresh snow), SWCRF is negative.

In Fig. 13 we have shown the SW cloud forcing from ERBE and INSAT. INSAT(new) indicates the bias corrected data. Clear sky albedo was calculated using Rank method. The pattern of SWCRF from both INSAT

and ERBE is found to be similar wherever ERBE data is available. The estimates of SWCRF from INSAT and ERBE are within 10 Wm^{-2} in most regions. Note again that INSAT is able to provide clear sky data in regions where ERBE has no clear sky data.

9. Net radiation

Net radiation is the measure of the net amount of energy available for the earth-atmosphere system. It is defined as

$$N = S(1 - \alpha) - F \quad (6)$$

Where, S is the incoming solar radiation at the TOA, α is the albedo and F is OLR.

Net radiation from INSAT was estimated using the OLR and albedo data sets generated in the previous sections. Data for incoming solar radiation was taken from ERBS since INSAT did not provide measurements of this parameter. A set of 10°×10° sub-regions from the total area was chosen for net radiation comparison. Table 4(a) shows the RMS error in net radiation between ERBS and other data sets for three such selected sub-regions. We have shown the error between ERBS and NOAA10 to depict the range of error inherent in ERBE data introduced due to different crossing time of these satellites over a place. INSAT(new) indicates that we used new OLR data set and INSAT albedo bias was corrected. INSAT(old) stands for old OLR set and without bias corrected albedo over ocean. Note that RMS error in net radiation for December 1988 and March 1989 in the Saudi Arabian region between INSAT(new) and ERBS is less than that between ERBS and NOAA10. Same feature can be noticed for the same months over south Indian Ocean region. RMS errors in NOAA10 and INSAT(new) when compared to ERBS for the Bay of Bengal region are comparable. Error in net radiation can originate from the error in absorbed solar radiation and error in OLR [first and second terms of Eqn. (6), respectively]. To understand the relative contribution of these two terms to the error in net radiation we have listed the RMS errors in absorbed solar radiation and OLR for the same regions and same months in Tables 4(b&c). To calculate the absorbed solar radiation we used the incoming solar radiation value from ERBS for all the cases. Therefore, difference in this term follows the difference in albedo only. In Table 4(b), INSAT(old) refers to the original INSAT albedo data and INSAT(new) refers to the bias corrected INSAT albedo data. Notice that the large error in NOAA10 net radiation is mainly because of the large error in absorbed solar radiation in December 1988 and March 1989 in the Saudi Arabian region, where INSAT(old or new) is closer to ERBS. Over south Indian Ocean relatively large error in INSAT(new) net radiation is on account of errors in OLR. In all cases difference between INSAT(old) and ERBS is higher than the error inherent in the ERBE data.

10. Net cloud radiative forcing

Net effect of cloud on the radiation balance of the earth-atmosphere system is termed as net cloud radiative forcing (or simply CRF) which can be written as

$$CRF = SWCRF + LWCRF \quad (7)$$

where SWCRF and LWCRF are SW and LW cloud radiative forcing respectively. As these two parameters are opposite in sign (Eqns. 5 and 4), net cloud forcing is less in magnitude than its individual components. Fig. 14 shows the spatial distribution of net CRF from ERBE and INSAT. INSAT(old) refers to old INSAT OLR and original INSAT albedo data. INSAT(new) stands for the new INSAT OLR and bias corrected INSAT albedo over ocean. Large negative CRF (~30-50 Wm^{-2}) can be noticed over cloud covered TCZ regions in both the months. In general, the pattern of the INSAT(new) CRF is closer to ERBE than INSAT(old) CRF. Similar pattern of net CRF was also noticed for January 1989.

11. Conclusion

We have studied the radiation budget in the Indian region using INSAT-1B data. Two of the three radiation budget components, *viz*. OLR and albedo, were estimated using INSAT data. INSAT-1B did not provide measurement of the third component, namely, the incident solar radiation at the TOA because INSAT-1B did not have a solar monitor. We have used ERBE measurements of this quantity in our study. The constants for conversion of brightness temperature to flux equivalent temperature were obtained by minimising the RMS error between ERBE and INSAT for May 1988 in the Indian region. The new set of constants of the empirical relation decreases the error in the estimates of OLR from INSAT brightness temperature data when compared to the previous set used by Arkin *et al*. (1989). As an example, the area mean RMS error for the old set for the month July 1988 was 19.1 Wm^{-2} and that for the new set was 10.7 Wm^{-2}. Error in INSAT OLR compared to ERBE was found to be related with the number of INSAT IR images available for that month. Broadband albedo of INSAT was found to be systematically lower than that of ERBS over ocean. It was shown that the bias can be removed by adding 2% to INSAT albedo over ocean, which substantially reduces the ERBS-INSAT RMS error in albedo. It was argued that the main source of error in INSAT albedo was the assumption of isotropic reflection in the algorithm of narrowband to broadband conversion of INSAT visible data. A bi-

spectral algorithm was used to identify clear sky and was found to provide a better estimate of clear sky albedo than a method that uses only visible data. We have shown that the effect of sun glint over ocean can introduce error in the estimates of monthly mean clear sky albedo if only one image per day is used. Net radiation calculated using the new OLR data set along with the bias corrected albedo over ocean was in good agreement with ERBS broadband estimates. We have demonstrated that operational satellites such as INSAT that carry narrowband sensors can provide a reasonable accurate estimate of various radiation budget parameters. There is, however, a need to tune some of the parameters used for the conversion of narrowband fluxes to broadband fluxes. These tuning parameters will vary from region to region. Hence the accuracy achieved in the narrow to broadband conversion in the Indian region may not be attained in other regions of the world.

Acknowledgements

The authors wish to thank Prof. V Ramanathan of Scripps Institute of Oceanography, San Diego, California for advice on the use of the INSAT-1B pixel data. We thank Indian Space Research Organisation for supporting this study under grant ISTC/AS/JS/601.

References

Abel, P. G. and Gruber, A., 1979, "An improved model for the calculation of longwave flux at 11 μm", NOAA Tech. Memo. NESS 106. Washington, DC, NTIS PB80-119431, 24.

Arkin, P. A., Krishnarao, A. V. R. and Kelkar, R. R., 1989, "Large scale precipitation and outgoing longwave radiation from INSAT-1B during the 1986 southwest monsoon season", *J. Clim*., **2**, 619-628.

Barkstrom, B. R., 1984, "The Earth Radiation Budget Experiment (ERBE)", *Bull. Amer. Meteor. Soc*., **65**, 1170-1185.

Barkstrom, B. R., Harrison, E. F., Smith, G., Green, R., Kibler, J., Cess, R. and the ERBE Science Team, 1989, "Earth Radiation Budget Experiment (ERBE) Archival and April 1985 results", *Bull. Amer. Meteor. Soc*., **70**, 1254-1262.

Bergman, J. W. and Salby, H. L., 1997, "The role of cloud diurnal variations in the time-mean energy budget", *J. Clim*., **10**, 1114-1124.

Gruber, A., Ruff, I. and Earnest, C., 1983, "Determination of planetary radiation budget from TIROS N satellites", NOAA technical report, NESDIS 3.

Gruber, A., Ellingson, R., Ardanuy, P., Weiss, M., Yang, S. K. and Oh, S. N., 1994, "A comparison of AVHRR and ERBE longwave flux estimates", *Bull. Amer. Meteor. Soc*., **75**, 2115-2130.

Harrison, E. F., Brooks, D. R., Minnis, P., Wielicki, B. A., Staylor, W. F., Gibson, G. G., Young, D. F., Denn, F. M. and the ERBE Science Team, 1988, "First estimates of diurnal variation of longwave radiation from the multiple satellite Earth Radiation Budget Experiment (ERBE)", *Bull. Amer. Meteor. Soc*., **69**, 1144-1151.

Kyle, H. L., Hicky, J. R., Ardanuy, P. E., Jacobowitz, H., Arking, A., Campbell, G. G., House, F. B., Maschhoff, R., Smith, G. L., Stowe, L. L. and Vonder Haar, T., 1993, "The Nimbus Earth Radiation Budget Experiment: 1975-1992", *Bull. Amer. Meteor. Soc*., **74**, 815-830.

Lamm, J. E., Smith, E. A., Mehta, A. V. and Jenne, R., 1991, "Description of the U.S. INSAT satellite data set (April 1984 to April 1989)", Special report prepared under NSF grant ATM-8812411.

Ramanathan, V., 1987, "The role of earth radiation budget studies in climate and general circulation research", *J. Geophyl. Res*., **92**, 4075-4095.

Ramanathan, V., Cess, R. D., Harrison, E. F., Minnis, P., Barkstrom, B. R., Ahmad, E. and Hartmann, D., 1989, "Cloud-radiative forcing and climate: Results from the Earth Radiation Budget Experiment. Science, **243**, 57-63.

Smith, E. A., 1984, "Radiative forcing of southwest summer monsoon", Ph.D. Dissertation, Dept. of Atmos. Sci., Colo. State Uni., Fort Collins, CO, p520.